

Improved measurement of the branching fractions of the inclusive decays $D^+ \rightarrow K_S^0 X$ and $D^0 \rightarrow K_S^0 X$

- M. Ablikim¹, M. N. Achasov^{12,b}, P. Adlarson⁷², M. Albrecht⁴, R. Aliberti³³, A. Amoroso^{71A,71C}, M. R. An³⁷, Q. An^{68,55}, Y. Bai⁵⁴, O. Bakina³⁴, R. Baldini Ferroli^{27A}, I. Balossino^{28A}, Y. Ban^{44,g}, V. Batozskaya^{1,42}, D. Becker³³, K. Begzsuren³⁰, N. Berger³³, M. Bertani^{27A}, D. Betttoni^{28A}, F. Bianchi^{71A,71C}, E. Bianco^{71A,71C}, J. Bloms⁶⁵, A. Bortone^{71A,71C}, I. Boyko³⁴, R. A. Briere⁵, A. Brueggemann⁶⁵, H. Cai⁷³, X. Cai^{1,55}, A. Calcaterra^{27A}, G. F. Cao^{1,60}, N. Cao^{1,60}, S. A. Cetin^{59A}, J. F. Chang^{1,55}, W. L. Chang^{1,60}, G. R. Che⁴¹, G. Chelkov^{34,a}, C. Chen⁴¹, Chao Chen⁵², G. Chen¹, H. S. Chen^{1,60}, M. L. Chen^{1,55,60}, S. J. Chen⁴⁰, S. M. Chen⁵⁸, T. Chen^{1,60}, X. R. Chen^{29,60}, X. T. Chen^{1,60}, Y. B. Chen^{1,55}, Z. J. Chen^{24,h}, W. S. Cheng^{71C}, S. K. Choi⁵², X. Chu⁴¹, G. Cibinetto^{28A}, F. Cossio^{71C}, J. J. Cui⁴⁷, H. L. Dai^{1,55}, J. P. Dai⁷⁶, A. Dbeysi¹⁸, R. E. de Boer⁴, D. Dedovich³⁴, Z. Y. Deng¹, A. Denig³³, I. Denysenko³⁴, M. Destefanis^{71A,71C}, F. De Mori^{71A,71C}, Y. Ding³², Y. Ding³⁸, J. Dong^{1,55}, L. Y. Dong^{1,60}, M. Y. Dong^{1,55,60}, X. Dong⁷³, S. X. Du⁷⁸, Z. H. Duan⁴⁰, P. Egorov^{34,a}, Y. L. Fan⁷³, J. Fang^{1,55}, S. S. Fang^{1,60}, W. X. Fang¹, Y. Fang¹, R. Farinelli^{28A}, L. Fava^{71B,71C}, F. Feldbauer⁴, G. Felici^{27A}, C. Q. Feng^{68,55}, J. H. Feng⁵⁶, K. Fischer⁶⁶, M. Fritsch⁴, C. Fritzsch⁶⁵, C. D. Fu¹, H. Gao⁶⁰, Y. N. Gao^{44,g}, Yang Gao^{68,55}, S. Garbolino^{71C}, I. Garzia^{28A,28B}, P. T. Ge⁷³, Z. W. Ge⁴⁰, C. Geng⁵⁶, E. M. Gersabeck⁶⁴, A. Gilman⁶⁶, K. Goetzen¹³, L. Gong³⁸, W. X. Gong^{1,55}, W. Gradl³³, M. Greco^{71A,71C}, L. M. Gu⁴⁰, M. H. Gu^{1,55}, Y. T. Gu¹⁵, C. Y. Guan^{1,60}, A. Q. Guo^{29,60}, L. B. Guo³⁹, R. P. Guo⁴⁶, Y. P. Guo^{11,f}, A. Guskov^{34,a}, W. Y. Han³⁷, X. Q. Hao¹⁹, F. A. Harris⁶², K. K. He⁵², K. L. He^{1,60}, F. H. Heinssius⁴, C. H. Heinz³³, Y. K. Heng^{1,55,60}, C. Herold⁵⁷, G. Y. Hou^{1,60}, Y. R. Hou⁶⁰, Z. L. Hou¹, H. M. Hu^{1,60}, J. F. Hu^{53,i}, T. Hu^{1,55,60}, Y. Hu¹, G. S. Huang^{68,55}, K. X. Huang⁵⁶, L. Q. Huang^{29,60}, X. T. Huang⁴⁷, Y. P. Huang¹, Z. Huang^{44,g}, T. Hussain⁷⁰, N. Hüsken^{26,33}, W. Imoehl²⁶, M. Irshad^{68,55}, J. Jackson²⁶, S. Jaeger⁴, S. Janchiv³⁰, E. Jang⁵², J. H. Jeong⁵², Q. Ji¹, Q. P. Ji¹⁹, X. B. Ji^{1,60}, X. L. Ji^{1,55}, Y. Y. Ji⁴⁷, Z. K. Jia^{68,55}, P. C. Jiang^{44,g}, S. S. Jiang³⁷, X. S. Jiang^{1,55,60}, Y. Jiang⁶⁰, J. B. Jiao⁴⁷, Z. Jiao²², S. Jin⁴⁰, Y. Jin⁶³, M. Q. Jing^{1,60}, T. Johansson⁷², S. Kabana³¹, N. Kalantar-Nayestanaki⁶¹, X. L. Kang⁹, X. S. Kang³⁸, R. Kappert⁶¹, M. Kavatsyuk⁶¹, B. C. Ke⁷⁸, I. K. Keshk⁴, A. Khoukaz⁶⁵, R. Kiuchi¹, R. Kliemt¹³, L. Koch³⁵, O. B. Kolcu^{59A}, B. Kopf⁴, M. Kuemmel⁴, M. Kuessner⁴, A. Kupsc^{42,72}, W. Kühn³⁵, J. J. Lane⁶⁴, J. S. Lange³⁵, P. Larin¹⁸, A. Lavania²⁵, L. Lavezzi^{71A,71C}, T. T. Lei^{68,k}, Z. H. Lei^{68,55}, H. Leithoff³³, M. Lellmann³³, T. Lenz³³, C. Li⁴¹, C. Li⁴⁵, C. H. Li³⁷, Cheng Li^{68,55}, D. M. Li⁷⁸, F. Li^{1,55}, G. Li¹, H. Li^{68,55}, H. B. Li^{1,60}, H. J. Li¹⁹, H. N. Li^{53,i}, Hui Li⁴¹, J. Q. Li⁴, J. S. Li⁵⁶, J. W. Li⁴⁷, Ke Li¹, L. J. Li^{1,60}, L. K. Li¹, Lei Li³, M. H. Li⁴¹, P. R. Li^{36,j,k}, S. X. Li¹¹, S. Y. Li⁵⁸, T. Li⁴⁷, W. D. Li^{1,60}, W. G. Li¹, X. H. Li^{68,55}, X. L. Li⁴⁷, Xiaoyu Li^{1,60}, Y. G. Li^{44,g}, Z. X. Li¹⁵, Z. Y. Li⁵⁶, C. Liang⁴⁰, H. Liang³², H. Liang^{1,60}, H. Liang^{68,55}, Y. F. Liang⁵¹, Y. T. Liang^{29,60}, G. R. Liao¹⁴, L. Z. Liao⁴⁷, J. Libby²⁵, A. Limphirat⁵⁷, D. X. Lin^{29,60}, T. Lin¹, B. J. Liu¹, C. Liu³², C. X. Liu¹, D. Liu^{18,68}, F. H. Liu⁵⁰, Fang Liu¹, Feng Liu⁶, G. M. Liu^{53,i}, H. Liu^{36,j,k}, H. B. Liu¹⁵, H. M. Liu^{1,60}, Huanhuan Liu¹, Huihui Liu²⁰, J. B. Liu^{68,55}, J. L. Liu⁶⁹, J. Y. Liu^{1,60}, K. Liu¹, K. Y. Liu³⁸, Ke Liu²¹, L. Liu^{68,55}, L. C. Liu²¹, Lu Liu⁴¹, M. H. Liu^{11,f}, P. L. Liu¹, Q. Liu⁶⁰, S. B. Liu^{68,55}, T. Liu^{11,f}, W. K. Liu⁴¹, W. M. Liu^{68,55}, X. Liu^{36,j,k}, Y. Liu^{36,j,k}, Y. B. Liu⁴¹, Z. A. Liu^{1,55,60}, Z. Q. Liu⁴⁷, X. C. Lou^{1,55,60}, F. X. Lu⁵⁶, H. J. Lu²², J. G. Lu^{1,55}, X. L. Lu¹, Y. Lu⁷, Y. P. Lu^{1,55}, Z. H. Lu^{1,60}, C. L. Luo³⁹, M. X. Luo⁷⁷, T. Luo^{11,f}, X. L. Luo^{1,55}, X. R. Lyu⁶⁰, Y. F. Lyu⁴¹, F. C. Ma³⁸, H. L. Ma¹, L. L. Ma⁴⁷, M. M. Ma^{1,60}, Q. M. Ma¹, R. Q. Ma^{1,60}, R. T. Ma⁶⁰, X. Y. Ma^{1,55}, Y. Ma^{44,g}, F. E. Maas¹⁸, M. Maggiora^{71A,71C}, S. Maldaner⁴, S. Malde⁶⁶, Q. A. Malik⁷⁰, A. Mangoni^{27B}, Y. J. Mao^{44,g}, Z. P. Mao¹, S. Marcello^{71A,71C}, Z. X. Meng⁶³, J. G. Messchendorp^{13,61}, G. Mezzadri^{28A}, H. Miao^{1,60}, T. J. Min⁴⁰, R. E. Mitchell²⁶, X. H. Mo^{1,55,60}, N. Yu. Muchnoi^{12,b}, Y. Nefedov³⁴, F. Nerling^{18,d}, I. B. Nikolaev^{12,b}, Z. Ning^{1,55}, S. Nisar^{10,l}, Y. Niu⁴⁷, S. L. Olsen⁶⁰, Q. Ouyang^{1,55,60}, S. Pacetti^{27B,27C}, X. Pan⁵², Y. Pan⁵⁴, A. Pathak³², Y. P. Pei^{68,55}, M. Pelizaeus⁴, H. P. Peng^{68,55}, K. Peters^{13,d}, J. L. Ping³⁹, R. G. Ping^{1,60}, S. Plura³³, S. Pogodin³⁴, V. Prasad^{68,55}, F. Z. Qi¹, H. Qi^{68,55}, H. R. Qi⁵⁸, M. Qi⁴⁰, T. Y. Qi^{11,f}, S. Qian^{1,55}, W. B. Qian⁶⁰, Z. Qian⁵⁶, C. F. Qiao⁶⁰, J. J. Qin⁶⁹, L. Q. Qin¹⁴, X. P. Qin^{11,f}, X. S. Qin⁴⁷, Z. H. Qin^{1,55}, J. F. Qiu¹, S. Q. Qu⁵⁸, K. H. Rashid⁷⁰, C. F. Redmer³³, K. J. Ren³⁷, A. Rivetti^{71C}, V. Rodin⁶¹, M. Rolo^{71C}, G. Rong^{1,60}, Ch. Rosner¹⁸, S. N. Ruan⁴¹, A. Sarantsev^{34,c}, Y. Schelhaas³³, C. Schnier⁴, K. Schoenning⁷², M. Scodeggio^{28A,28B}, K. Y. Shan^{11,f}, W. Shan²³, X. Y. Shan^{68,55}, J. F. Shangguan⁵², L. G. Shao^{1,60}, M. Shao^{68,55}, C. P. Shen^{11,f}, H. F. Shen^{1,60}, W. H. Shen⁶⁰, X. Y. Shen^{1,60}, B. A. Shi⁶⁰, H. C. Shi^{68,55}, J. Y. Shi¹, Q. Q. Shi⁵², R. S. Shi^{1,60}, X. Shi^{1,55}, J. J. Song¹⁹, W. M. Song^{32,1}, Y. X. Song^{44,g}, S. Sosio^{71A,71C}, S. Spataro^{71A,71C}, F. Stieler³³, P. P. Su⁵², Y. J. Su⁶⁰, G. X. Sun¹, H. Sun⁶⁰, H. K. Sun¹, J. F. Sun¹⁹, L. Sun⁷³, S. S. Sun^{1,60}, T. Sun^{1,60}, W. Y. Sun³², Y. J. Sun^{68,55}, Y. Z. Sun¹, Z. T. Sun⁴⁷, Y. X. Tan^{68,55}, C. J. Tang⁵¹, G. Y. Tang¹, J. Tang⁵⁶, Y. A. Tang⁷³, L. Y. Tao⁶⁹,

Q. T. Tao^{24,h}, M. Tat⁶⁶, J. X. Teng^{68,55}, V. Thoren⁷², W. H. Tian⁴⁹, Y. Tian^{29,60}, I. Uman^{59B}, B. Wang¹,
 B. Wang^{68,55}, B. L. Wang⁶⁰, C. W. Wang⁴⁰, D. Y. Wang^{44,g}, F. Wang⁶⁹, H. J. Wang^{36,j,k}, H. P. Wang^{1,60},
 K. Wang^{1,55}, L. L. Wang¹, M. Wang⁴⁷, Meng Wang^{1,60}, S. Wang¹⁴, S. Wang^{11,f}, T. Wang^{11,f}, T. J. Wang⁴¹,
 W. Wang⁵⁶, W. H. Wang⁷³, W. P. Wang^{68,55}, X. Wang^{44,g}, X. F. Wang^{36,j,k}, X. L. Wang^{11,f}, Y. Wang⁵⁸,
 Y. D. Wang⁴³, Y. F. Wang^{1,55,60}, Y. H. Wang⁴⁵, Y. Q. Wang¹, Yaqian Wang^{17,1}, Z. Wang^{1,55}, Z. Y. Wang^{1,60},
 Ziyi Wang⁶⁰, D. H. Wei¹⁴, F. Weidner⁶⁵, S. P. Wen¹, D. J. White⁶⁴, U. Wiedner⁴, G. Wilkinson⁶⁶, M. Wolke⁷²,
 L. Wollenberg⁴, J. F. Wu^{1,60}, L. H. Wu¹, L. J. Wu^{1,60}, X. Wu^{11,f}, X. H. Wu³², Y. Wu⁶⁸, Y. J. Wu²⁹, Z. Wu^{1,55},
 L. Xia^{68,55}, T. Xiang^{44,g}, D. Xiao^{36,j,k}, G. Y. Xiao⁴⁰, H. Xiao^{11,f}, S. Y. Xiao¹, Y. L. Xiao^{11,f}, Z. J. Xiao³⁹,
 C. Xie⁴⁰, X. H. Xie^{44,g}, Y. Xie⁴⁷, Y. G. Xie^{1,55}, Y. H. Xie⁶, Z. P. Xie^{68,55}, T. Y. Xing^{1,60}, C. F. Xu^{1,60},
 C. J. Xu⁵⁶, G. F. Xu¹, H. Y. Xu⁶³, Q. J. Xu¹⁶, X. P. Xu⁵², Y. C. Xu⁷⁵, Z. P. Xu⁴⁰, F. Yan^{11,f}, L. Yan^{11,f},
 W. B. Yan^{68,55}, W. C. Yan⁷⁸, H. J. Yang^{48,e}, H. L. Yang³², H. X. Yang¹, Tao Yang¹, Y. F. Yang⁴¹, Y. X. Yang^{1,60},
 Yifan Yang^{1,60}, M. Ye^{1,55}, M. H. Ye⁸, J. H. Yin¹, Z. Y. You⁵⁶, B. X. Yu^{1,55,60}, C. X. Yu⁴¹, G. Yu^{1,60}, T. Yu⁶⁹,
 X. D. Yu^{44,g}, C. Z. Yuan^{1,60}, L. Yuan², S. C. Yuan¹, X. Q. Yuan¹, Y. Yuan^{1,60}, Z. Y. Yuan⁵⁶, C. X. Yue³⁷,
 A. A. Zafar⁷⁰, F. R. Zeng⁴⁷, X. Zeng⁶, Y. Zeng^{24,h}, X. Y. Zhai³², Y. H. Zhan⁵⁶, A. Q. Zhang^{1,60}, B. L. Zhang^{1,60},
 B. X. Zhang¹, D. H. Zhang⁴¹, G. Y. Zhang¹⁹, H. Zhang⁶⁸, H. H. Zhang⁵⁶, H. H. Zhang³², H. Q. Zhang^{1,55,60},
 H. Y. Zhang^{1,55}, J. J. Zhang⁴⁹, J. L. Zhang⁷⁴, J. Q. Zhang³⁹, J. W. Zhang^{1,55,60}, J. X. Zhang^{36,j,k}, J. Y. Zhang¹,
 J. Z. Zhang^{1,60}, Jianyu Zhang^{1,60}, Jiawei Zhang^{1,60}, L. M. Zhang⁵⁸, L. Q. Zhang⁵⁶, Lei Zhang⁴⁰, P. Zhang¹,
 Q. Y. Zhang^{37,78}, Shuihan Zhang^{1,60}, Shulei Zhang^{24,h}, X. D. Zhang⁴³, X. M. Zhang¹, X. Y. Zhang⁴⁷,
 X. Y. Zhang⁵², Y. Zhang⁶⁶, Y. T. Zhang⁷⁸, Y. H. Zhang^{1,55}, Yan Zhang^{68,55}, Yao Zhang¹, Z. H. Zhang¹,
 Z. L. Zhang³², Z. Y. Zhang⁴¹, Z. Y. Zhang⁷³, G. Zhao¹, J. Zhao³⁷, J. Y. Zhao^{1,60}, J. Z. Zhao^{1,55}, Lei Zhao^{68,55},
 Ling Zhao¹, M. G. Zhao⁴¹, S. J. Zhao⁷⁸, Y. B. Zhao^{1,55}, Y. X. Zhao^{29,60}, Z. G. Zhao^{68,55}, A. Zhemchugov^{34,a},
 B. Zheng⁶⁹, J. P. Zheng^{1,55}, Y. H. Zheng⁶⁰, B. Zhong³⁹, C. Zhong⁶⁹, X. Zhong⁵⁶, H. Zhou⁴⁷, L. P. Zhou^{1,60},
 X. Zhou⁷³, X. K. Zhou⁶⁰, X. R. Zhou^{68,55}, X. Y. Zhou³⁷, Y. Z. Zhou^{11,f}, J. Zhu⁴¹, K. Zhu¹, K. J. Zhu^{1,55,60},
 L. X. Zhu⁶⁰, S. H. Zhu⁶⁷, S. Q. Zhu⁴⁰, W. J. Zhu^{11,f}, Y. C. Zhu^{68,55}, Z. A. Zhu^{1,60}, J. H. Zou¹, J. Zu^{68,55}

(BESIII Collaboration)

¹ Institute of High Energy Physics, Beijing 100049, People's Republic of China

² Beihang University, Beijing 100191, People's Republic of China

³ Beijing Institute of Petrochemical Technology, Beijing 102617, People's Republic of China

⁴ Bochum Ruhr-University, D-44780 Bochum, Germany

⁵ Carnegie Mellon University, Pittsburgh, Pennsylvania 15213, USA

⁶ Central China Normal University, Wuhan 430079, People's Republic of China

⁷ Central South University, Changsha 410083, People's Republic of China

⁸ China Center of Advanced Science and Technology, Beijing 100190, People's Republic of China

⁹ China University of Geosciences, Wuhan 430074, People's Republic of China

¹⁰ COMSATS University Islamabad, Lahore Campus, Defence Road, Off Raiwind Road, 54000 Lahore, Pakistan

¹¹ Fudan University, Shanghai 200433, People's Republic of China

¹² G.I. Budker Institute of Nuclear Physics SB RAS (BINP), Novosibirsk 630090, Russia

¹³ GSI Helmholtzcentre for Heavy Ion Research GmbH, D-64291 Darmstadt, Germany

¹⁴ Guangxi Normal University, Guilin 541004, People's Republic of China

¹⁵ Guangxi University, Nanning 530004, People's Republic of China

¹⁶ Hangzhou Normal University, Hangzhou 310036, People's Republic of China

¹⁷ Hebei University, Baoding 071002, People's Republic of China

¹⁸ Helmholtz Institute Mainz, Staudinger Weg 18, D-55099 Mainz, Germany

¹⁹ Henan Normal University, Xinxiang 453007, People's Republic of China

²⁰ Henan University of Science and Technology, Luoyang 471003, People's Republic of China

²¹ Henan University of Technology, Zhengzhou 450001, People's Republic of China

²² Huangshan College, Huangshan 245000, People's Republic of China

²³ Hunan Normal University, Changsha 410081, People's Republic of China

²⁴ Hunan University, Changsha 410082, People's Republic of China

²⁵ Indian Institute of Technology Madras, Chennai 600036, India

²⁶ Indiana University, Bloomington, Indiana 47405, USA

²⁷ INFN Laboratori Nazionali di Frascati , (A)INFN Laboratori Nazionali di Frascati, I-00044, Frascati, Italy;
 (B)INFN Sezione di Perugia, I-06100, Perugia, Italy; (C)University of Perugia, I-06100, Perugia, Italy

- ²⁸ INFN Sezione di Ferrara, (A)INFN Sezione di Ferrara, I-44122, Ferrara, Italy; (B)University of Ferrara, I-44122, Ferrara, Italy
- ²⁹ Institute of Modern Physics, Lanzhou 730000, People's Republic of China
- ³⁰ Institute of Physics and Technology, Peace Avenue 54B, Ulaanbaatar 13330, Mongolia
- ³¹ Instituto de Alta Investigación, Universidad de Tarapacá, Casilla 7D, Arica, Chile
- ³² Jilin University, Changchun 130012, People's Republic of China
- ³³ Johannes Gutenberg University of Mainz, Johann-Joachim-Becher-Weg 45, D-55099 Mainz, Germany
- ³⁴ Joint Institute for Nuclear Research, 141980 Dubna, Moscow region, Russia
- ³⁵ Justus-Liebig-Universitaet Giessen, II. Physikalisches Institut, Heinrich-Buff-Ring 16, D-35392 Giessen, Germany
- ³⁶ Lanzhou University, Lanzhou 730000, People's Republic of China
- ³⁷ Liaoning Normal University, Dalian 116029, People's Republic of China
- ³⁸ Liaoning University, Shenyang 110036, People's Republic of China
- ³⁹ Nanjing Normal University, Nanjing 210023, People's Republic of China
- ⁴⁰ Nanjing University, Nanjing 210093, People's Republic of China
- ⁴¹ Nankai University, Tianjin 300071, People's Republic of China
- ⁴² National Centre for Nuclear Research, Warsaw 02-093, Poland
- ⁴³ North China Electric Power University, Beijing 102206, People's Republic of China
- ⁴⁴ Peking University, Beijing 100871, People's Republic of China
- ⁴⁵ Qufu Normal University, Qufu 273165, People's Republic of China
- ⁴⁶ Shandong Normal University, Jinan 250014, People's Republic of China
- ⁴⁷ Shandong University, Jinan 250100, People's Republic of China
- ⁴⁸ Shanghai Jiao Tong University, Shanghai 200240, People's Republic of China
- ⁴⁹ Shanxi Normal University, Linfen 041004, People's Republic of China
- ⁵⁰ Shanxi University, Taiyuan 030006, People's Republic of China
- ⁵¹ Sichuan University, Chengdu 610064, People's Republic of China
- ⁵² Soochow University, Suzhou 215006, People's Republic of China
- ⁵³ South China Normal University, Guangzhou 510006, People's Republic of China
- ⁵⁴ Southeast University, Nanjing 211100, People's Republic of China
- ⁵⁵ State Key Laboratory of Particle Detection and Electronics, Beijing 100049, Hefei 230026, People's Republic of China
- ⁵⁶ Sun Yat-Sen University, Guangzhou 510275, People's Republic of China
- ⁵⁷ Suranaree University of Technology, University Avenue 111, Nakhon Ratchasima 30000, Thailand
- ⁵⁸ Tsinghua University, Beijing 100084, People's Republic of China
- ⁵⁹ Turkish Accelerator Center Particle Factory Group, (A)Istinye University, 34010, Istanbul, Turkey; (B)Near East University, Nicosia, North Cyprus, Mersin 10, Turkey
- ⁶⁰ University of Chinese Academy of Sciences, Beijing 100049, People's Republic of China
- ⁶¹ University of Groningen, NL-9747 AA Groningen, The Netherlands
- ⁶² University of Hawaii, Honolulu, Hawaii 96822, USA
- ⁶³ University of Jinan, Jinan 250022, People's Republic of China
- ⁶⁴ University of Manchester, Oxford Road, Manchester, M13 9PL, United Kingdom
- ⁶⁵ University of Muenster, Wilhelm-Klemm-Strasse 9, 48149 Muenster, Germany
- ⁶⁶ University of Oxford, Keble Road, Oxford OX13RH, United Kingdom
- ⁶⁷ University of Science and Technology Liaoning, Anshan 114051, People's Republic of China
- ⁶⁸ University of Science and Technology of China, Hefei 230026, People's Republic of China
- ⁶⁹ University of South China, Hengyang 421001, People's Republic of China
- ⁷⁰ University of the Punjab, Lahore-54590, Pakistan
- ⁷¹ University of Turin and INFN, (A)University of Turin, I-10125, Turin, Italy; (B)University of Eastern Piedmont, I-15121, Alessandria, Italy; (C)INFN, I-10125, Turin, Italy
- ⁷² Uppsala University, Box 516, SE-75120 Uppsala, Sweden
- ⁷³ Wuhan University, Wuhan 430072, People's Republic of China
- ⁷⁴ Xinyang Normal University, Xinyang 464000, People's Republic of China
- ⁷⁵ Yantai University, Yantai 264005, People's Republic of China
- ⁷⁶ Yunnan University, Kunming 650500, People's Republic of China

⁷⁷ Zhejiang University, Hangzhou 310027, People's Republic of China

⁷⁸ Zhengzhou University, Zhengzhou 450001, People's Republic of China

^a Also at the Moscow Institute of Physics and Technology, Moscow 141700, Russia

^b Also at the Novosibirsk State University, Novosibirsk, 630090, Russia

^c Also at the NRC "Kurchatov Institute", PNPI, 188300, Gatchina, Russia

^d Also at Goethe University Frankfurt, 60323 Frankfurt am Main, Germany

^e Also at Key Laboratory for Particle Physics, Astrophysics and Cosmology, Ministry of Education; Shanghai Key Laboratory for Particle Physics and Cosmology; Institute of Nuclear and Particle Physics, Shanghai 200240, People's Republic of China

^f Also at Key Laboratory of Nuclear Physics and Ion-beam Application (MOE) and Institute of Modern Physics, Fudan University, Shanghai 200443, People's Republic of China

^g Also at State Key Laboratory of Nuclear Physics and Technology, Peking University, Beijing 100871, People's Republic of China

^h Also at School of Physics and Electronics, Hunan University, Changsha 410082, China

ⁱ Also at Guangdong Provincial Key Laboratory of Nuclear Science, Institute of Quantum Matter, South China Normal University, Guangzhou 510006, China

^j Also at Frontiers Science Center for Rare Isotopes, Lanzhou University, Lanzhou 730000, People's Republic of China

^k Also at Lanzhou Center for Theoretical Physics, Lanzhou University, Lanzhou 730000, People's Republic of China

^l Also at the Department of Mathematical Sciences, IBA, Karachi , Pakistan

By analyzing 2.93 fb^{-1} of e^+e^- collision data taken at the center-of-mass energy of 3.773 GeV with the BESIII detector, the branching fractions of the inclusive decays $D^+ \rightarrow K_S^0 X$ and $D^0 \rightarrow K_S^0 X$ are measured to be $(32.78 \pm 0.13 \pm 0.27)\%$ and $(20.54 \pm 0.12 \pm 0.18)\%$, respectively, where the first uncertainties are statistical and the second are systematic. These results are consistent with the world averages of previous measurements, but with improved precision.

PACS numbers: 13.20.Fc, 14.40.Lb

I. INTRODUCTION

Weak decays of charmed mesons offer an ideal laboratory for improving our understanding of both strong and weak interactions. The D^+ and D^0 mesons decay dominantly into final states involving K^- and \bar{K}^0 via Cabibbo-favored processes. The branching fractions of the inclusive decays $D^{+(0)} \rightarrow K^0/\bar{K}^0 X$, where X denotes any possible particle combinations, were first measured by Mark-III [1] in 1991 and later by BES [2] in 2006. Assuming $\mathcal{B}(K^0/\bar{K}^0 \rightarrow K_S^0) = 0.5$ and considering the world average branching fractions of $D^{+(0)} \rightarrow K^0/\bar{K}^0 X$, the branching fractions of $D^{+(0)} \rightarrow K_S^0 X$ are expected to be $(30.5 \pm 2.5)\%$ and $(23.5 \pm 2.0)\%$, respectively [3]. In recent years, the precision of the branching fractions of known decay modes has been significantly improved, and many new channels have been observed. Following this progress, the sum of the branching fractions of the exclusive D^+ and D^0 decays involving K_S^0 are found to be $(31.68 \pm 0.32)\%$ and $(18.16 \pm 0.72)\%$, as summarized in Appendix A. In contrast, however, the branching fractions of the inclusive decays $D^+ \rightarrow K_S^0 X$ and $D^0 \rightarrow K_S^0 X$ suffer from large uncertainties due to the limited samples sizes used to perform the measurements. Improved determinations of these inclusive decay branching fractions will help to quantify and guide the search for the missing decay modes involving a K_S^0 meson.

In this paper, we report the improved measurements of the branching fractions of $D^+ \rightarrow K_S^0 X$ and $D^0 \rightarrow K_S^0 X$, obtained from the analysis of 2.93 fb^{-1} of e^+e^- collision data [4] taken at the center-of-mass energy \sqrt{s} of 3.773 GeV with the BESIII detector. The charge-conjugated processes are implied throughout the discussion.

II. BESIII DETECTOR AND MONTE CARLO SIMULATION

The BESIII detector [5] records symmetric e^+e^- collisions provided by the BEPCII storage ring [6], which operates in the center-of-mass energy range from 2.0 to 4.95 GeV, with a peak luminosity of $1 \times 10^{33} \text{ cm}^{-2}\text{s}^{-1}$ achieved at $\sqrt{s} = 3.773$ GeV. BESIII has collected large data samples in this energy region [7]. The cylindrical core of the BESIII detector covers 93% of the full solid angle and consists of a helium-based multilayer drift chamber (MDC), a plastic scintillator time-of-flight system (TOF), and a CsI(Tl) electromagnetic calorimeter (EMC), which are all enclosed in a superconducting solenoidal magnet providing a 1.0 T magnetic field. [8] The solenoid is supported by an octagonal flux-return yoke with resistive plate counter muon identification modules interleaved with steel. The charged-particle momentum resolution at $1 \text{ GeV}/c$ is 0.5%, and the specific energy loss (dE/dx)

resolution is 6% for electrons from Bhabha scattering. The EMC measures photon energies with a resolution of 2.5% (5%) at 1 GeV in the barrel (end-cap) region. The time resolution in the TOF barrel region is 68 ps, while that in the end-cap region is 110 ps.

Simulated samples produced with the GEANT4-based [9] Monte Carlo (MC) package, which includes the geometric description of the BESIII detector and the detector response, are used to determine the detection efficiency and to estimate the backgrounds. The simulation includes the beam-energy spread and initial-state radiation in the e^+e^- annihilations modeled with the generator KKMC [10]. The inclusive MC samples consist of the production of $D\bar{D}$ pairs with consideration of quantum coherence for all neutral D modes, the non- $D\bar{D}$ decays of the $\psi(3770)$, the initial-state radiation production of the J/ψ and $\psi(3686)$ states, and the continuum processes. The known decay modes are modeled with EVTGEN [11] using the branching fractions taken from Particle Data Group (PDG) [3], and the remaining unknown decays of the charmonium states are modeled by LUNDCHARM [12]. Final-state radiation from charged final-state particles is incorporated using the PHOTOS package [13].

The three-body decays $D^+ \rightarrow K_S^0\pi^+\pi^0$ and $D^+ \rightarrow K_S^0\pi^+\eta$ are modeled with a modified data-driven generator BODY3 [11], which was developed to simulate different intermediate states in data for a given three-body final state. The Dalitz plot from data, corrected for backgrounds and efficiencies, is taken as input for the BODY3 generator. The decay $D^+ \rightarrow K_S^0\pi^+\pi^+\pi^-$ is modeled with the partial-wave analysis model from Ref. [14]. Other decays reported in recent BESIII measurements [15–17] are modeled by constructing a cocktail of possible intermediate resonances.

III. ANALYSIS METHOD

At $\sqrt{s} = 3.773$ GeV, $D^0\bar{D}^0$ or D^+D^- pairs are produced without accompanying hadron(s), thereby offering a clean environment in which to investigate hadronic D decays with the double-tag (DT) method [18]. To measure the branching fractions of the hadronic decays of $D^+(D^0)$ mesons, as a first step the single-tag $D^-(\bar{D}^0)$ mesons are selected by using the hadronic decay modes $D^- \rightarrow K^+\pi^-\pi^-$ and $\bar{D}^0 \rightarrow K^+\pi^-$. The number of the expected single-tag $D^- (\bar{D}^0)$ mesons is given by

$$N_{\text{tag}} = 2N_{D\bar{D}}\mathcal{B}_{\text{tag}}\epsilon_{\text{tag}}, \quad (1)$$

where $N_{D\bar{D}}$ is the total number of $D^+D^- (D^0\bar{D}^0)$ pairs, \mathcal{B}_{tag} is the branching fraction of $D^- (\bar{D}^0)$ decay into the tag mode, and ϵ_{tag} is the efficiency of reconstructing the single-tag $D^- (\bar{D}^0)$ mesons.

The double-tag sample is comprised of events in which the signal decay $D^{+(0)} \rightarrow K_S^0X$ can be selected in the presence of the single-tag $D^- (\bar{D}^0)$ mesons. The number

of the expected double-tag events is given by

$$N_{\text{DT}} = 2N_{D\bar{D}}\mathcal{B}_{\text{tag}}\mathcal{B}_{\text{sig}}\epsilon_{\text{DT}}, \quad (2)$$

where \mathcal{B}_{sig} is the branching fraction of $D^{+(0)} \rightarrow K_S^0X$, and ϵ_{DT} is the efficiency of detecting the double-tag events. The branching fraction of the signal decay is then

$$\mathcal{B}_{\text{sig}} = \frac{N_{\text{DT}}}{N_{\text{tag}}\epsilon_{\text{sig}}}, \quad (3)$$

where $\epsilon_{\text{sig}} = \frac{\epsilon_{\text{DT}}}{\epsilon_{\text{tag}}}$ is the effective efficiency of reconstructing $D^{+(0)} \rightarrow K_S^0X$.

Quantum correlations between the $D^0\bar{D}^0$ pair modify the double-tag rates. The measured branching fraction of $D^0 \rightarrow K_S^0X$ tagged by $\bar{D}^0 \rightarrow K^+\pi^-$ must be corrected to

$$\mathcal{B}_{\text{sig}}^{\text{cor}} = \frac{1}{1 - C_f(2f_{CP+} - 1)}\mathcal{B}_{\text{sig}}, \quad (4)$$

where f_{CP+} is the fractional CP -even content of the decay $D^0 \rightarrow K_S^0X$, and C_f is the strong-phase factor

$$C_f = \frac{2r \cos \delta}{1 + r^2}. \quad (5)$$

Here $r = 0.0587 \pm 0.0002$ [21] is the ratio between doubly-Cabibbo-suppressed and Cabibbo-favored amplitudes for $D^0/\bar{D}^0 \rightarrow K^\pm\pi^\mp$, and $\delta = (191.7^{+3.6}_{-3.8})^\circ$ [21] is the strong-phase difference between two amplitudes [22, 23]. These inputs yield $C_f = (-11.5 \pm 0.2)\%$ for $D^0/\bar{D}^0 \rightarrow K^\pm\pi^\mp$.

The CP -even fraction f_{CP+} of $D^0 \rightarrow K_S^0X$ decays is not known, but can be measured from the $D^0\bar{D}^0$ data set. Following Refs. [19, 20], the CP -even fraction is calculated by

$$f_{CP\pm} = \frac{N^\pm}{N^+ + N^-},$$

$$N^\pm = \frac{M^\pm_{\text{measured}}}{S^\pm},$$

and

$$S_\pm = \frac{S^\pm_{\text{measured}}}{1 - \eta_\pm y_D},$$

where N^\pm is the ratio between double-tag and single-tag yields with CP -odd(even) tags, M^\pm_{measured} is the number of double-tag candidates for a signal channel versus CP -odd(even) tags, S^\pm_{measured} is the number of single-tag candidates for CP -even(odd) decay modes, S^\pm is the number of the corrected single-tag candidates for CP -even(odd) decay modes. Finally, $\eta_\pm = \pm 1$ for CP -even(odd) mode and $y_D = (6.47 \pm 0.24) \times 10^{-3}$ is the mixing parameter taken from the latest average from HFLAV [21].

IV. YIELDS OF SINGLE-TAG D^- (\bar{D}^0) MESONS

Charged kaons and charged pions are selected with the same selection criteria as those used in our previous works [24–26]. All charged tracks, apart from those from K_S^0 decays, are required to have a polar angle θ with respect to the MDC symmetry axis within the MDC acceptance $|\cos\theta| < 0.93$, a distance of closest approach with respect to the interaction point along the beam direction $|V_z| < 10$ cm, and a distance of closest approach with respect to the interaction point in the plane transverse to the beam direction $|V_{xy}| < 1$ cm. Particle identification (PID) for charged kaons and pions is performed by exploiting combined dE/dx and TOF information. The confidence levels for pion and kaon hypotheses (CL_π and CL_K) are calculated. Charged tracks satisfying $CL_K > CL_\pi$ and $CL_\pi > CL_K$ are assigned as charged kaons and pions, respectively.

When selecting $\bar{D}^0 \rightarrow K^+\pi^-$ candidates, contamination from cosmic rays and Bhabha events is suppressed with the following requirements [27]. First, the two charged tracks must have a TOF time difference less than 5 ns and they must be inconsistent with being a muon-antimuon or an electron-positron pair. Second, in the event there must be at least one EMC shower with an energy greater than 50 MeV or at least one additional charged track detected in the MDC.

The tagged D^- (\bar{D}^0) mesons are identified using the energy difference $\Delta E \equiv E_{\bar{D}} - E_{\text{beam}}$ and the beam-constrained mass $M_{\text{BC}} \equiv \sqrt{E_{\text{beam}}^2 - |\vec{p}_{\bar{D}}|^2}$. Here, E_{beam} is the beam energy, and $\vec{p}_{\bar{D}}$ and $E_{\bar{D}}$ are the momentum and energy of the D^- (\bar{D}^0) candidate in the rest frame of e^+e^- system, respectively. For each tag mode, if there are multiple candidates in an event, only the one with the smallest $|\Delta E|$ is kept. The tagged \bar{D} candidates are required to be within $\Delta E \in (-25, 25)$ MeV.

To determine the yields of single-tag D^- (\bar{D}^0) mesons for individual tag modes, binned maximum-likelihood fits are performed on the corresponding M_{BC} distributions of the accepted single-tag candidates [24–26]. In the fits, the D^- (\bar{D}^0) signal is modeled by an MC-simulated shape convolved with a double-Gaussian function describing the resolution difference between data and MC simulation. The combinatorial background is described by an ARGUS function [28]. The best fit results for the M_{BC} distributions are shown in Fig. 1. The yields of the single-tag D^- and \bar{D}^0 mesons are 798935 ± 1011 and 529227 ± 761 respectively, where the uncertainties are statistical only. The efficiencies of reconstructing the single-tag D^- (\bar{D}^0) mesons are estimated to be $(51.90 \pm 0.08)\%$ and $(65.60 \pm 0.09)\%$ respectively, by analyzing the inclusive MC sample.

V. YIELDS OF DOUBLE-TAG $D^{+(0)}$ MESONS

The K_S^0 mesons are reconstructed in the $K_S^0 \rightarrow \pi^+\pi^-$ decay mode. The charged pions making up the K_S^0

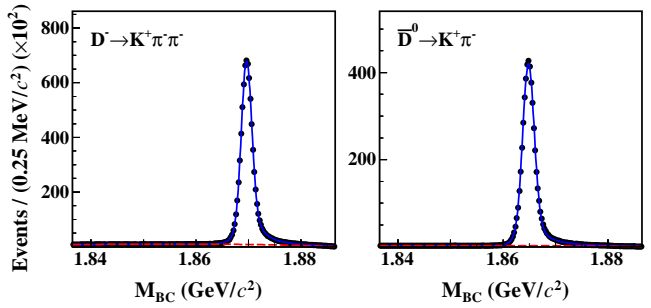


Fig. 1. Best fits to the M_{BC} distributions of the single-tag candidates for $D^- \rightarrow K^+\pi^-\pi^-$ and $\bar{D}^0 \rightarrow K^+\pi^-$. The points with error bars are data. The blue solid curves are the fit results. The red dashed curves are the fitted combinatorial background shapes.

candidates are required to satisfy $|V_z| < 20$ cm and $|\cos\theta| < 0.93$. To improve the resolution of the K_S^0 invariant mass, a primary vertex and a K_S^0 decay vertex fit are performed on the $\pi^+\pi^-$ pairs. To suppress the combinatorial background, we require $L/\sigma_L > 2$, where σ_L is the uncertainty of the flight distance L . The invariant mass of the chosen charged pions, $M_{\pi^+\pi^-}$, is required to be within $|M_{\pi^+\pi^-} - M_{K_S^0}| < 12$ MeV/c², which corresponds to about $\pm 3\sigma$ around the known K_S^0 mass ($M_{K_S^0}$) [3]. To estimate the combinatorial $\pi^+\pi^-$ background, the K_S^0 sideband region is defined by $20 < |M_{\pi^+\pi^-} - M_{K_S^0}| < 44$ MeV/c², which corresponds to about $\pm 5\sigma$ to $\pm 11\sigma$ away from the known K_S^0 mass. The definitions of the K_S^0 signal and sideband regions are indicated in Fig. 2. The background is mainly from the $D\bar{D}$ and $q\bar{q}$ ($q = u, d, s$) continuum process. Especially, events with wrong tag and one real K_S^0 meson will form a peak in the $M_{\pi^+\pi^-}$ distribution but do not form a peak in the M_{BC} distribution. There are some discrepancy in resolution between data and MC simulation and this effect will be taken into account in the systematic uncertainty of K_S^0 reconstruction.

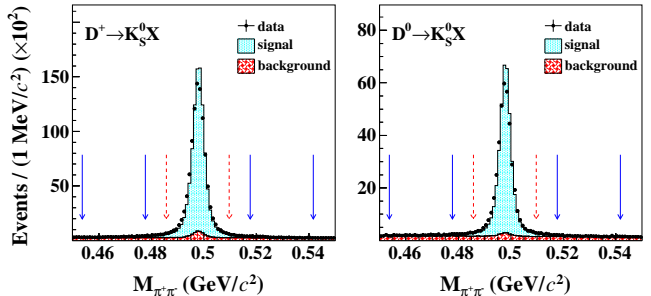


Fig. 2. Distributions of $M_{\pi^+\pi^-}$ of the candidates for $D^+ \rightarrow K_S^0 X$ and $D^0 \rightarrow K_S^0 X$. The red dashed and blue solid arrow pairs show the K_S^0 signal and sideband regions, respectively. The points with error bars are data. The histograms are the inclusive MC sample.

The distributions of the recoil mass, momentum, and $\cos\theta$ of the K_S^0 candidates from the selected $D^+ \rightarrow K_S^0 X$ and $D^0 \rightarrow K_S^0 X$ events are shown in Fig. 3. The experimental and the MC distributions are in good agreement.

The decay yields of the signal are determined from the fits to the M_{BC} distributions of the accepted double-tag events in data. However, combinatorial background events with $M_{\pi^+\pi^-}$ in the K_S^0 signal region may form peaking background in the M_{BC} distribution. So, the net signal yields are determined by

$$N_{DT}^{\text{net}} = N_{K_S^0 \text{sig}} - f_{co} \cdot N_{K_S^0 \text{sb}}, \quad (6)$$

where $N_{K_S^0 \text{sig}}$ and $N_{K_S^0 \text{sb}}$ are the fitted double-tag yields in the K_S^0 signal and sideband regions, respectively; the sideband scaling factor f_{co} is taken as 0.5 under the assumption that the background contribution in the $M_{\pi^+\pi^-}$ spectrum is flat. Figure 4 shows the M_{BC} distributions of the accepted double-tag events in data with $M_{\pi^+\pi^-}$ in the K_S^0 signal and sideband regions. We perform similar fits to these spectra as for the fits to the single-tag candidates. In these fits, the parameters of the smeared double-Gaussian resolution functions are fixed at the values obtained from the fits to the single-tag $D^- (\bar{D}^0)$ candidates. The fit results are also shown in Fig. 4. From these fits, we obtain the yields of $N_{K_S^0 \text{sig}}$ and $N_{K_S^0 \text{sb}}$, as summarized in Table 2.

The efficiencies of reconstructing the inclusive decays $D^{+(0)} \rightarrow K_S^0 X$ are determined by analyzing the inclusive MC sample (ϵ_{sig}). Inserting the numbers of N_{DT}^{net} , N_{tag} , and ϵ_{sig} into Eq. (3), we obtain the branching fractions of $D^+ \rightarrow K_S^0 X$ and $D^0 \rightarrow K_S^0 X$.

In order to account for the effect of quantum correlations on the branching fraction of $D^0 \rightarrow K_S^0 X$, we apply the correction given in Eq. 4. This procedure requires knowledge of the CP -even fraction of these decays, which is measured in the data by using the CP -even tag $\bar{D}^0 \rightarrow K^+ K^-$ and the CP -odd tag $\bar{D}^0 \rightarrow K_S^0 \pi^0$. The yields of these tags and the resulting value for f_{CP+} are given in Table 1. The correction factor is determined to be 1.0204 ± 0.0024 .

Table 1. Measurements of S_{measured}^\pm , M_{measured}^\pm , f_{CP+} and the correction factor for $D^0 \rightarrow K_S^0 X$ due to quantum correlation effect.

CP tag mode	$\bar{D}^0 \rightarrow K^+ K^-$	$\bar{D}^0 \rightarrow K_S^0 \pi^0$
S_{measured}^\pm	57779 ± 287	70512 ± 311
M_{measured}^\pm	4760 ± 81	4068 ± 78
f_{CP+}		0.413 ± 0.010
Correction factor		1.0204 ± 0.0024

The net efficiencies, including all factors discussed above, and the final values for the branching fractions are summarized in Table 2.

VI. SYSTEMATIC UNCERTAINTIES

With the double-tag method, the branching-fraction measurements have a greatly reduced sensitivity to systematic bias arising from the selection criteria on the tag side.

The systematic uncertainties in the yields of the single-tag D^- or \bar{D}^0 mesons have been estimated in Refs. [24] to be 0.50%, by examining the relative change between data and MC simulation yields when varying the fit range, signal shape, and end point of the ARGUS function.

The data/MC difference of the K_S^0 reconstruction is determined to be $(1.01 \pm 0.53)\%$ by using control samples of $J/\psi \rightarrow K_S^0 K^\pm \pi^\mp$ and $\phi K_S^0 K^\pm \pi^\mp$ decays [29]. After correcting the MC efficiencies to match those in data, we assign 0.53% as the systematic uncertainty per K_S^0 decay.

Two methods are used to estimate the systematic uncertainty associated with the K_S^0 multiplicity. Firstly, we vary the components of the decays containing one, two, and three K_S^0 mesons by $\pm 1\sigma$ according to their known branching fractions. The changes in the detection efficiencies for $D^+ \rightarrow K_S^0 X$ and $D^0 \rightarrow K_S^0 X$, 0.05% and 0.07% respectively, are assigned as the uncertainties. Secondly, we measure the detection efficiencies for all known exclusive decays and determine the change of the re-weighted detection efficiency by varying each of decays within $\pm 1\sigma$ according to the known branching fractions. By adding in quadrature all the changes in the detection efficiencies, we obtain 0.20% for $D^+ \rightarrow K_S^0 X$ and 0.28% for $D^0 \rightarrow K_S^0 X$, which are assigned as the uncertainties. We assign the larger effect coming from the two methods as the corresponding systematic uncertainty for each signal decay.

To estimate the systematic uncertainty due to the choice of the K_S^0 sideband region, we examine the effects on the branching fractions by shifting the K_S^0 sideband region by ± 2 or ± 4 MeV/ c^2 . If the difference of the re-measured branching fraction is greater than the statistical uncertainty after considering the signal correlations, it is assigned as the systematic uncertainty; otherwise, it is neglected. Following this procedure, we assign 0.15% for $D^+ \rightarrow K_S^0 X$ and 0.10% for $D^0 \rightarrow K_S^0 X$ as the corresponding systematic uncertainties.

The uncertainty on the correction factor for quantum correlations is propagated to the branching fraction of $D^0 \rightarrow K_S^0 X$ decays. The uncertainties due to the limited signal double-tag MC samples for $D^+ \rightarrow K_S^0 X$ and $D^0 \rightarrow K_S^0 X$ are estimated to be 0.25% and 0.28%, respectively. The uncertainty of the branching fraction of $K_S^0 \rightarrow \pi^+ \pi^-$ is 0.07%, taken from the PDG [3].

The uncertainty arising from the scale factor f_{co} used in Eq. (6) is assessed with the alternative scale factors derived from the inclusive MC sample, which are 0.549 and 0.534 for $D^+ \rightarrow K_S^0 X$ and $D^0 \rightarrow K_S^0 X$, respectively. The changes of the re-measured branching fractions, 0.02% and 0.05%, are assigned as the corresponding systematic uncertainties.

The systematic uncertainties are summarized in

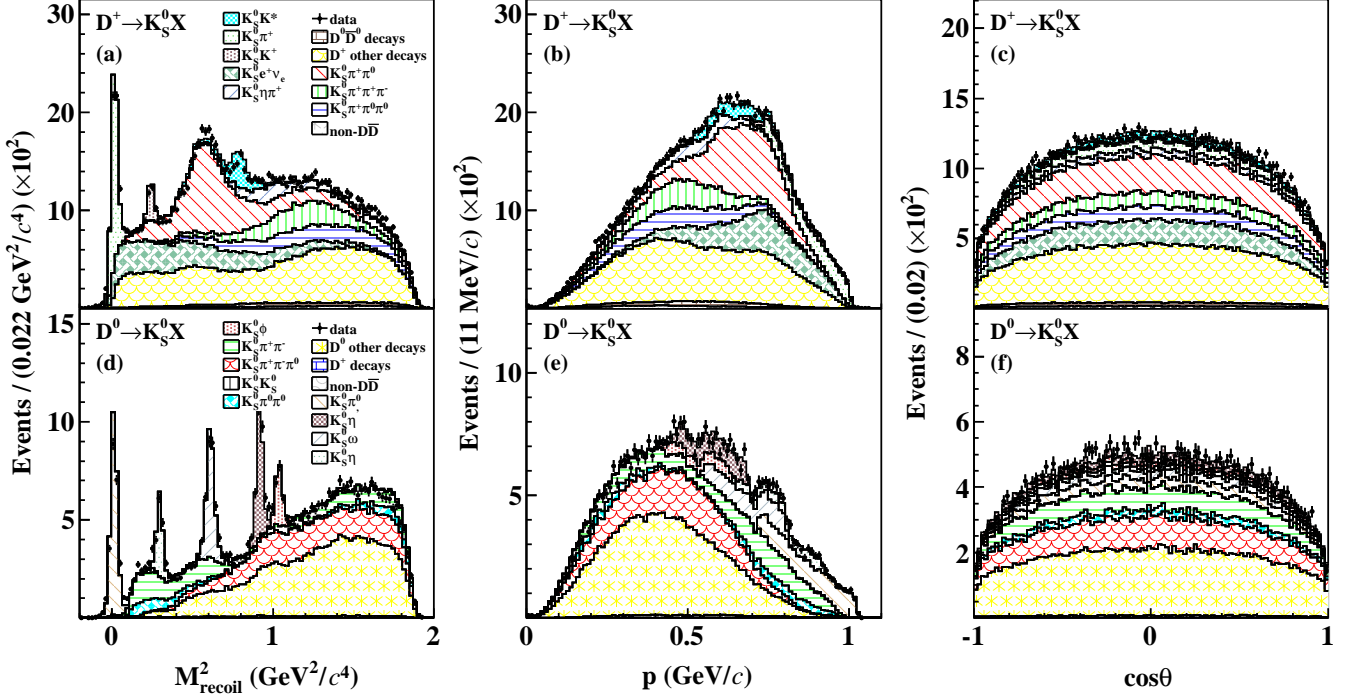


Fig. 3. Distributions of the (a,d) recoil mass, (b,e) momentum, and (c,f) $\cos \theta$ of the K_S^0 candidates from the accepted candidates for $D^+ \rightarrow K_S^0 X$ and $D^0 \rightarrow K_S^0 X$. The points with error bars are data. The histograms are the inclusive MC sample.

Table 2. Numbers of single-tag D^- (\bar{D}^0) mesons (N_{tag}), fitted double-tag yields in the K_S^0 signal and sideband regions ($N_{K_S^0 \text{sig}}$ and $N_{K_S^0 \text{sb}}$), net numbers of signal events ($N_{\text{DT}}^{\text{net}}$), efficiencies of finding $D^{+(0)} \rightarrow K_S^0 X$ in the presence of the single-tag D^- (\bar{D}^0) meson (ϵ_{sig}), and measured branching fractions of $D^{+(0)} \rightarrow K_S^0 X$ (\mathcal{B}_{sig}). The efficiency values include the branching fraction of $K_S^0 \rightarrow \pi^+ \pi^-$ as well as the correction factors described in the text. The uncertainties are statistical only.

Signal mode	N_{tag}	$N_{K_S^0 \text{sig}}$	$N_{K_S^0 \text{sb}}$	$N_{\text{DT}}^{\text{net}}$	$\epsilon_{\text{sig}} (\%)$	$\mathcal{B}_{\text{sig}} (\%)$
$D^+ \rightarrow K_S^0 X$	798935 ± 1011	102186 ± 365	13981 ± 140	95195 ± 372	36.35 ± 0.08	32.78 ± 0.13
$D^0 \rightarrow K_S^0 X$	529227 ± 761	42166 ± 215	8688 ± 97	37822 ± 220	34.81 ± 0.10	20.54 ± 0.12

Table 3. Assuming that all these components are independent, they are summed in quadrature to give the totals 0.82% and 0.87% for the branching fractions of $D^+ \rightarrow K_S^0 X$ and $D^0 \rightarrow K_S^0 X$, respectively.

VII. SUMMARY

By analyzing 2.93 fb^{-1} of e^+e^- collision data taken at the center-of-mass energy of 3.773 GeV with the BESIII detector, the branching fractions of $D^+ \rightarrow K_S^0 X$ and $D^0 \rightarrow K_S^0 X$ are measured to be $(32.78 \pm 0.13 \pm 0.27)\%$ and $(20.54 \pm 0.12 \pm 0.18)\%$, respectively, where the first uncertainties are statistical and the second are systematic. These results are consistent with previous measurements by Mark-III [1] and BES [2] within uncertainties, as summarized in Table 4. Compared with the average values from the PDG, the precision

Table 3. Relative systematic uncertainties (in %) in the branching fraction measurements. A “...” denotes that there is no systematic uncertainty.

Source	$D^+ \rightarrow K_S^0 X$	$D^0 \rightarrow K_S^0 X$
N_{tag}	0.50	0.50
K_S^0 reconstruction	0.53	0.53
K_S^0 multiplicity	0.20	0.28
K_S^0 sideband	0.15	0.10
Quantum-correlation effect	...	0.24
MC statistics	0.25	0.28
Quoted branching fraction	0.07	0.07
Scale factor f_{co}	0.02	0.05
Total	0.82	0.87

Table 4. Comparisons of the branching fractions of $D^{+(0)} \rightarrow K_S^0 X$ measured in this study and Mark-III, BES, and PDG. For the values from BES, Mark-III, and PDG, we take half of the branching fractions of $D \rightarrow K^0/\bar{K}^0 X$. $\mathcal{B}_{\text{exclusive}}^{\text{sum}}$ denotes the total branching fractions summing over all known exclusive $D^{+(0)}$ decays involving a K_S^0 .

Decay mode	Mark-III (%) [1]	BES (%) [2]	PDG (%) [3]	This study (%)	$\mathcal{B}_{\text{exclusive}}^{\text{sum}} (\%)$
$D^+ \rightarrow K_S^0 X$	$30.60 \pm 3.25 \pm 2.15$	$30.25 \pm 2.75 \pm 1.65$	30.5 ± 2.5	$32.78 \pm 0.13 \pm 0.27$	31.68 ± 0.32
$D^0 \rightarrow K_S^0 X$	$22.75 \pm 2.50 \pm 1.60$	$23.80 \pm 2.40 \pm 1.50$	23.5 ± 2.0	$20.54 \pm 0.12 \pm 0.18$	18.16 ± 0.72

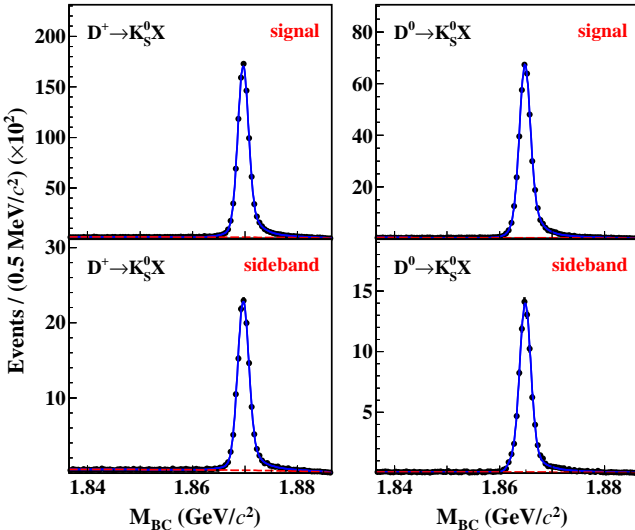


Fig. 4. Best fits to the M_{BC} distributions of the double-tag events in data. The upper and lower plots correspond to events with $M_{\pi^+\pi^-}$ in the K_S^0 signal and sideband regions, respectively. The points with error bars are data, the blue solid curves are the fit results, the red dashed curves are the fitted combinatorial background shapes.

of the branching fractions of $D^+ \rightarrow K_S^0 X$ and $D^0 \rightarrow K_S^0 X$ is improved by factors of 9.0 and 8.1, respectively. Summing over the branching fractions of the known $D^{+(0)}$ decay modes containing K_S^0 , we obtain $\mathcal{B}_{\text{exclusive}}^{\text{sum}}(D^+ \rightarrow K_S^0 X) = (31.68 \pm 0.32)\%$ and $\mathcal{B}_{\text{exclusive}}^{\text{sum}}(D^0 \rightarrow K_S^0 X) = (18.16 \pm 0.72)\%$. The differences between the inclusive and exclusive decay branching fractions are $(1.10 \pm 0.41)\%$ and $(2.38 \pm 0.75)\%$ for D^+ and D^0 decays, respectively. These results indicate that there may be some missing decay modes involving K_S^0 for both D^+ and D^0 yet to be observed.

VIII. ACKNOWLEDGEMENT

The BESIII collaboration thanks the staff of BEPCII and the IHEP computing center for their strong support. This work is supported in part by National Key R&D Program of China under Contracts Nos. 2020YFA0406400, 2020YFA0406300; National Natural Science Foundation of China (NSFC) under Contracts Nos. 11635010, 11735014, 11835012, 11935015, 11935016, 11935018, 11961141012, 12022510, 12025502, 12035009, 12035013, 12192260, 12192261, 12192262, 12192263, 12192264, 12192265; the Chinese Academy of Sciences (CAS) Large-Scale Scientific Facility Program; Joint Large-Scale Scientific Facility Funds of the NSFC and CAS under Contract No. U1832207, U1932102; the CAS Center for Excellence in Particle Physics (CCEPP); 100 Talents Program of CAS; The Institute of Nuclear and Particle Physics (INPAC) and Shanghai Key Laboratory for Particle Physics and Cosmology; ERC under Contract No. 758462; European Union's Horizon 2020 research and innovation programme under Marie Skłodowska-Curie grant agreement under Contract No. 894790; German Research Foundation DFG under Contracts Nos. 443159800, Collaborative Research Center CRC 1044, GRK 2149; Istituto Nazionale di Fisica Nucleare, Italy; Ministry of Development of Turkey under Contract No. DPT2006K-120470; National Science and Technology fund; National Science Research and Innovation Fund (NSRF) via the Program Management Unit for Human Resources & Institutional Development, Research and Innovation under Contract No. B16F640076; STFC (United Kingdom); Suranaree University of Technology (SUT), Thailand Science Research and Innovation (TSRI), and National Science Research and Innovation Fund (NSRF) under Contract No. 160355; The Royal Society, UK under Contracts Nos. DH140054, DH160214; The Swedish Research Council; U. S. Department of Energy under Contract No. DE-FG02-05ER41374.

Appendix A: Branching fractions of the known exclusive $D^{+(0)}$ decays involving K_S^0

Tables 5 and 6 summarize the branching fractions of the known exclusive D^+ and D^0 decays involving K_S^0 , respectively.

Table 5. Initial and final states contributing to the inclusive decay $D^+ \rightarrow K_S^0 X$ and the corresponding branching fractions.

Initial state	\mathcal{B} (%)	Final state	\mathcal{B} (%)
$K_S^0\pi^+$	1.49 ± 0.03 [30]	$K_S^0\pi^+$	1.49 ± 0.03
$\bar{K}^0e^+\nu_e$	8.73 ± 0.10 [3]	$K_S^0e^+\nu_e$	4.37 ± 0.05
$\bar{K}^{*0}e^+\nu_e$	5.40 ± 0.10 [3]	$K_S^0\pi^0e^+\nu_e$	0.89 ± 0.02
$\bar{K}^0\mu^+\nu_\mu$	8.76 ± 0.19 [3]	$K_S^0\mu^+\nu_\mu$	4.380 ± 0.095
$\bar{K}^{*0}\mu^+\nu_\mu$	5.27 ± 0.15 [3]	$K_S^0\pi^0\mu^+\nu_\mu$	0.88 ± 0.02
$K_S^0K_S^0K^+$	0.254 ± 0.013 [3]	$K_S^0K_S^0K^+$	0.254 ± 0.013
$K_S^0K_L^0K^+$	0.508 ± 0.026 [3]	$K_S^0K_L^0K^+$	0.508 ± 0.026
$K_S^0K_S^0\pi^+$	0.270 ± 0.013 [3]	$K_S^0K_S^0\pi^+$	0.270 ± 0.013
$\bar{K}^0\pi^+\pi^+\pi^-$	6.20 ± 0.18 [3]	$K_S^0\pi^+\pi^+\pi^-$	3.10 ± 0.09
$\bar{K}^0K^+K^-\pi^+$	0.048 ± 0.010 [3]	$K_S^0K^+K^-\pi^+$	0.024 ± 0.005
$K_S^0\pi^+\pi^0$	7.36 ± 0.21 [3]	$K_S^0\pi^+\pi^0$	7.36 ± 0.21
\bar{K}^0K^{*+}	1.738 ± 0.182 [31]	$K_S^0K^{*+}$	0.869 ± 0.091
$\bar{K}_1^0(1270)e^+\nu_e$	0.231 ± 0.030 [32]	$K_S^0\pi^0\pi^0e^+\nu_e$	0.0055 ± 0.0007
$\bar{K}_1^0(1270)e^+\nu_e$	0.231 ± 0.030 [32]	$K_S^0\pi^+\pi^-e^+\nu_e$	0.039 ± 0.005
$\bar{K}_1^0(1270)\mu^+\nu_\mu$	0.231 ± 0.030 [32]	$K_S^0\pi^+\pi^-\mu^+\nu_\mu$	0.039 ± 0.005
$\bar{K}_1^0(1270)\mu^+\nu_\mu$	0.231 ± 0.030 [32]	$K_S^0\pi^0\pi^0\mu^+\nu_\mu$	0.0055 ± 0.0007
$K_S^0\pi^+\eta$	1.309 ± 0.048 [26]	$K_S^0\pi^+\eta$	1.309 ± 0.048
$K_S^0K^+\eta$	0.0185 ± 0.0050 [26]	$K_S^0K^+\eta$	0.0185 ± 0.0050
$K_S^0\pi^+\pi^0\eta$	0.12 ± 0.03 [26]	$K_S^0\pi^+\pi^0\eta$	0.12 ± 0.03
$K_S^0K^+\pi^+\pi^-$	0.189 ± 0.013 [15]	$K_S^0K^+\pi^+\pi^-$	0.189 ± 0.013
$K_S^0K^-\pi^+\pi^+$	0.227 ± 0.013 [15]	$K_S^0K^-\pi^+\pi^+$	0.227 ± 0.013
$K_S^0K^+\pi^0\pi^0$	0.058 ± 0.013 [15]	$K_S^0K^+\pi^0\pi^0$	0.058 ± 0.013
$K_S^0K_S^0\pi^+\pi^0$	0.134 ± 0.021 [15]	$K_S^0K_S^0\pi^+\pi^0$	0.134 ± 0.021
$K_S^0K_L^0\pi^+\pi^0$	0.268 ± 0.042 [15]	$K_S^0K_L^0\pi^+\pi^0$	0.268 ± 0.042
\bar{K}^0K^+	0.604 ± 0.024 [33]	$K_S^0K^+$	0.302 ± 0.012
$K_S^0K^+\pi^0$	0.507 ± 0.003 [33]	$K_S^0K^+\pi^0$	0.507 ± 0.003
$\phi\pi^+$	0.570 ± 0.015 [34]	$K_S^0K_L^0\pi^+$	0.193 ± 0.006
$\bar{K}^0\pi^+\eta'$	0.380 ± 0.042 [35]	$K_S^0\pi^+\eta'$	0.190 ± 0.021
$K_S^0\omega\pi^+$	0.707 ± 0.050 [16]	$K_S^0\omega\pi^+$	0.707 ± 0.050
$K_S^0\pi^+\pi^0\pi^0$	2.2516 ± 0.1068 [36]	$K_S^0\pi^+\pi^0\pi^0$	2.2516 ± 0.1068
$K_S^0\pi^+\pi^+\pi^-\pi^0$	0.4001 ± 0.0550 [36]	$K_S^0\pi^+\pi^+\pi^-\pi^0$	0.4001 ± 0.0550
$K_S^0\pi^+\pi^0\pi^0\pi^0$	0.126 ± 0.050 [36]	$K_S^0\pi^+\pi^0\pi^0\pi^0$	0.126 ± 0.050
$\phi\pi^+\pi^0$	0.579 ± 0.055 [37]	$K_S^0K_L^0\pi^+\pi^0$	0.196 ± 0.019
Sum	31.68 ± 0.32

- [1] D. Coffman *et al.* (Mark-III Collaboration), *Phys. Lett. B* **263**, 135 (1991).
- [2] M. Ablikim *et al.* (BES Collaboration), *Phys. Lett. B* **643**, 246 (2006).
- [3] R. L. Workman *et al.* (Particle Data Group), *Prog. Theor. Exp. Phys.* **2022**, 083C01 (2022).
- [4] M. Ablikim *et al.* (BESIII Collaboration), *Chin. Phys. C* **37**, 123001 (2013); *Phys. Lett. B* **753**, 629 (2016).
- [5] M. Ablikim *et al.* (BESIII Collaboration), *Nucl. Instrum. Meth. A* **614**, 345 (2010).
- [6] C. H. Yu *et al.*, Proceedings of IPAC2016, Busan, Korea, 2016.
- [7] M. Ablikim *et al.* (BESIII Collaboration), *Chin. Phys. C* **44**, 040001 (2020).
- [8] K. X. Huang, *et al.*, *Nucl. Sci. Tech.* **33**, 142 (2022).
- [9] S. Agostinelli *et al.* (GEANT4 Collaboration), *Nucl. Instrum. Meth. A* **506**, 250 (2003).
- [10] S. Jadach, B. F. L. Ward, and Z. Was, *Comp. Phys. Comm.* **130**, 260 (2000); *Phys. Rev. D* **63**, 113009 (2001).
- [11] D. J. Lange, *Nucl. Instrum. Meth. A* **462**, 152 (2001); R. G. Ping, *Chin. Phys. C* **32**, 599 (2008).
- [12] J. C. Chen, G. S. Huang, X. R. Qi, D. H. Zhang, and Y. S. Zhu, *Phys. Rev. D* **62**, 034003 (2000); R. L. Yang, R. G. Ping and H. Chen, *Chin. Phys. Lett.* **31**, 061301 (2014).
- [13] E. Richter-Was, *Phys. Lett. B* **303**, 163 (1993).
- [14] M. Ablikim *et al.* (BESIII Collaboration), *Phys. Rev. D* **100**, 072008 (2019).
- [15] M. Ablikim *et al.* (BESIII Collaboration), *Phys. Rev. D* **102**, 052006 (2020).

Table 6. Initial and final states contributing to the inclusive decay $D^0 \rightarrow K_S^0 X$ and the corresponding branching fractions.

Initial state	\mathcal{B} (%)	Final state	\mathcal{B} (%)
$K_S^0\omega$	1.11 ± 0.12 [3]	$K_S^0\omega$	1.11 ± 0.12
$K_S^0\eta'\pi^0$	0.252 ± 0.027 [3]	$K_S^0\eta'\pi^0$	0.252 ± 0.027
$K^-a_0^+$	0.059 ± 0.018 [3]	$K_S^0K^+K^-$	0.003 ± 0.001
$K_S^0\phi$	0.444 ± 0.015 [3]	$K_S^0\phi$	0.444 ± 0.015
ϕK_L^0	0.4440 ± 0.0304 [3]	$K_S^0K_L^0K_L^0$	0.151 ± 0.010
$\bar{K}^*\pi^0$	1.82 ± 0.07 [3]	$K_S^0\pi^0\pi^0$	0.303 ± 0.012
$\phi\gamma$	0.00282 ± 0.00019 [3]	$K_S^0K_L^0\gamma$	0.0010 ± 0.0001
$K_S^0\pi^+\pi^-$	2.80 ± 0.18 [3]	$K_S^0\pi^+\pi^-$	2.80 ± 0.18
$K_S^0K^+\pi^-$	0.217 ± 0.034 [3]	$K_S^0K^+\pi^-$	0.217 ± 0.034
$K_S^0K^-\pi^+$	0.33 ± 0.05 [3]	$K_S^0K^-\pi^+$	0.33 ± 0.05
$K_S^0K_S^0K^-\pi^+$	0.059 ± 0.013 [3]	$K_S^0K_S^0K^-\pi^+$	0.059 ± 0.013
$K_S^0K_L^0K^-\pi^+$	0.1180 ± 0.0013 [3]	$K_S^0K_L^0K^-\pi^+$	0.1180 ± 0.0013
$K_S^0K_S^0K^+\pi^-$	0.059 ± 0.013 [3]	$K_S^0K_S^0K^+\pi^-$	0.059 ± 0.013
$K_S^0K_L^0K^+\pi^-$	0.1180 ± 0.0013 [3]	$K_S^0K_L^0K^+\pi^-$	0.1180 ± 0.0013
$K_S^0\rho^0\pi^+\pi^-$	0.11 ± 0.07 [3]	$K_S^0\pi^+\pi^-\pi^+\pi^-$	0.11 ± 0.07
$K^*-\pi^+\pi^+\pi^-$	0.10 ± 0.07 [3]	$K_S^0\pi^+\pi^-\pi^+\pi^-$	0.033 ± 0.023
$K_S^0\pi^+\pi^-\pi^0$	4.09 ± 0.60 [3]	$K_S^0\pi^+\pi^-\pi^0$	4.09 ± 0.60
$\phi\pi^+\pi^-$	0.02 ± 0.01 [3]	$K_S^0K_L^0\pi^+\pi^-$	0.0068 ± 0.0034
$\bar{K}^*\pi^+\gamma$	0.042 ± 0.007 [3]	$K_S^0\pi^0\gamma$	0.007 ± 0.001
$K_S^0\pi^0\eta$	1.006 ± 0.046 [26]	$K_S^0\pi^0\eta$	1.006 ± 0.046
$K_S^0K_S^0\eta$	0.0130 ± 0.0062 [26]	$K_S^0K_S^0\eta$	0.0130 ± 0.0062
$K_S^0K_L^0\eta$	0.0270 ± 0.0124 [26]	$K_S^0K_L^0\eta$	0.0270 ± 0.0124
$K_S^0\pi^+\pi^-\eta$	0.280 ± 0.021 [26]	$K_S^0\pi^+\pi^-\eta$	0.280 ± 0.021
$K_S^0\pi^0\pi^0\eta$	0.176 ± 0.026 [26]	$K_S^0\pi^0\pi^0\eta$	0.176 ± 0.026
$K_S^0K^-\pi^+\pi^0$	0.132 ± 0.016 [15]	$K_S^0K^-\pi^+\pi^0$	0.132 ± 0.016
$K_S^0K_S^0\pi^+\pi^-$	0.053 ± 0.009 [15]	$K_S^0K_S^0\pi^+\pi^-$	0.053 ± 0.009
$K_S^0K_L^0\pi^+\pi^-$	0.106 ± 0.018 [15]	$K_S^0K_L^0\pi^+\pi^-$	0.106 ± 0.018
$K_S^0K^-\pi^+\pi^0$	0.132 ± 0.016 [15]	$K_S^0K^-\pi^+\pi^0$	0.132 ± 0.016
$K_S^0K^+\pi^-\pi^0$	0.065 ± 0.008 [15]	$K_S^0K^+\pi^-\pi^0$	0.065 ± 0.008
$\phi\pi^0$	0.117 ± 0.004 [34]	$K_S^0K_L^0\pi^0$	0.040 ± 0.001
$\phi\eta$	0.018 ± 0.005 [34]	$K_S^0K_L^0\eta$	0.006 ± 0.001
$K_S^0\pi^0\omega$	0.848 ± 0.055 [16]	$K_S^0\pi^0\omega$	0.848 ± 0.055
$K_S^0\pi^0\pi^0\pi^0$	0.591 ± 0.042 [36]	$K_S^0\pi^0\pi^0\pi^0$	0.591 ± 0.042
$K_S^0\pi^+\pi^-\pi^0\pi^0$	0.327 ± 0.045 [36]	$K_S^0\pi^+\pi^-\pi^0\pi^0$	0.327 ± 0.045
$K_S^0\eta'$	0.949 ± 0.016 [38]	$K_S^0\eta'$	0.949 ± 0.016
$K_S^0\pi^0$	1.240 ± 0.022 [38]	$K_S^0\pi^0$	1.240 ± 0.022
$K^*-e^+\nu_e$	2.03 ± 0.66 [39]	$K_S^0\pi^-e^+\nu_e$	0.68 ± 0.22
$\bar{K}^0\pi^-e^+\nu_e$	0.158 ± 0.034 [39]	$K_S^0\pi^-e^+\nu_e$	0.079 ± 0.017
$K^*-\mu^+\nu_\mu$	1.91 ± 0.62 [39]	$K_S^0\pi^-\mu^+\nu_\mu$	0.63 ± 0.20
$K_1^-(1270)e^+\nu_e$	0.109 ± 0.018 [40]	$K_S^0\pi^0\pi^-e^+\nu_e$	0.026 ± 0.004
$K_1^-(1270)\mu^+\nu_\mu$	0.109 ± 0.018 [40]	$K_S^0\pi^0\pi^-\mu^+\nu_\mu$	0.026 ± 0.004
$K_S^0K_S^0$	0.0170 ± 0.0015 [41]	$K_S^0K_S^0$	0.0170 ± 0.0015
$K_S^0K_S^0K_S^0$	0.072 ± 0.007 [41]	$K_S^0K_S^0K_S^0$	0.072 ± 0.007
$K_S^0K_L^0K_L^0$	0.216 ± 0.021 [41]	$K_S^0K_L^0K_L^0$	0.216 ± 0.021
$K_S^0K_S^0K_L^0$	0.216 ± 0.021 [41]	$K_S^0K_S^0K_L^0$	0.216 ± 0.021
Sum	18.16 ± 0.72

- [16] M. Ablikim *et al.* (BESIII Collaboration), *Phys. Rev. D* **105**, 032009 (2022).
- [17] M. Ablikim *et al.* (BESIII Collaboration), arXiv:2205.14031.
- [18] H. B. Li and X. R. Lyu, *Natl. Sci. Rev.* **8**, nwab181 (2021).
- [19] T. Evans *et al.*, *Phys. Lett. B* **757**, 520 (2016); *765*, 402(E) (2017).
- [20] M. Ablikim *et al.* (BESIII Collaboration), *Phys. Rev. D* **100**, 072006 (2019).
- [21] Heavy Flavor Averaging Group (HFLAV), (<http://www.slac.stanford.edu/xorg/hflav/charm/>).

- [22] T. Gershon, J. Libby, and G. Wilkinson, *Phys. Lett. B* **750**, 338 (2015).
- [23] T. Evans *et al.*, *Phys. Lett. B* **757**, 520 (2016); **765**, 402(E) (2017).
- [24] M. Ablikim *et al.* (BESIII Collaboration), *Phys. Rev. Lett.* **121**, 171803 (2018).
- [25] M. Ablikim *et al.* (BESIII Collaboration), *Phys. Rev. D* **101**, 052009 (2020).
- [26] M. Ablikim *et al.* (BESIII Collaboration), *Phys. Rev. Lett.* **124**, 241803 (2020).
- [27] M. Ablikim *et al.* (BESIII Collaboration), *Phys. Lett. B* **734**, 227 (2014).
- [28] H. Albrecht *et al.* (ARGUS Collaboration), *Phys. Lett. B* **241**, 278 (1990).
- [29] M. Ablikim *et al.* (BESIII Collaboration), *Phys. Rev. D* **92**, 112008 (2015).
- [30] C. Patrignani *et al.* (Particle Data Group), *Chin. Phys. C* **40**, 100001 (2016).
- [31] M. Ablikim *et al.* (BESIII Collaboration), *Phys. Rev. D* **104**, 012006 (2021).
- [32] M. Ablikim *et al.* (BESIII Collaboration), *Phys. Rev. Lett.* **123**, 231801 (2019).
- [33] M. Ablikim *et al.* (BESIII Collaboration), *Phys. Rev. D* **99**, 032002 (2019).
- [34] M. Ablikim *et al.* (BESIII Collaboration), *Phys. Lett. B* **798**, 135017 (2019).
- [35] M. Ablikim *et al.* (BESIII Collaboration), *Phys. Rev. D* **99**, 092009 (2018).
- [36] M. Ablikim *et al.* (BESIII Collaboration), *arXiv:2205.14031v1*.
- [37] M. Ablikim *et al.* (BESIII Collaboration), “Measurement of the branching fraction of $D^+ \rightarrow \phi\pi^+\pi^0$ ”, publication in preparation.
- [38] M. Ablikim *et al.* (BESIII Collaboration), *Phys. Rev. D* **97**, 072004 (2018).
- [39] M. Ablikim *et al.* (BESIII Collaboration), *Phys. Rev. D* **99**, 011103 (2019).
- [40] M. Ablikim *et al.* (BESIII Collaboration), *Phys. Rev. Lett.* **127**, 131801 (2021).
- [41] M. Ablikim *et al.* (BESIII Collaboration), *Phys. Lett. B* **765**, 231 (2017).